The Maturation-Dependent Conformational Change of the Major Capsid Protein of Bacteriophage T4 Involves a Substantial Change in Secondary Structure†

Alasdair C. Steven,*,‡ Heather Greenstone,‡ Adelia C. Bauer,‡ and Robert W. Williams§

Laboratory of Physical Biology, National Institute of Arthritis, Musculoskeletal and Skin Diseases, Bethesda, Maryland 20892, and Department of Biochemistry, Uniformed Services University of the Health Sciences, 4301 Jones Bridge Road, Bethesda, Maryland 20814

Received November 20, 1989; Revised Manuscript Received February 28, 1990

ABSTRACT: We have investigated the conformational basis of the expansion transformation that occurs upon maturation of the bacteriophage T4 prohead, by using laser Raman spectroscopy to determine the secondary structure of the major capsid protein in both the precursor and the mature states of the surface lattice. This transformation involves major changes in the physical, chemical, and immunological properties of the capsid and is preceded in vivo by processing of its major protein, gp23 (56 kDa), to gp23* (49 kDa), by proteolysis of its N-terminal gp23-Δ domain. The respective secondary structures of gp23 in the unexpanded state, and of gp23* in the expanded state, were determined from the laser Raman spectra of polyheads, tubular polymorphic variants of the capsid. Similar measurements were also made on uncleaved polyheads that had been expanded in vitro and, for reference, on thermally denatured polyheads. We find that, with or without cleavage of gp23, expansion is accompanied by substantial changes in secondary structure, involving a major reduction in α-helix content and an increase in β-sheet. The β-sheet contents of gp23* or gp23 in the expanded state of the surface lattice, and even of gp23 in the unexpanded state, are sufficient for a domain with the "jellyroll" fold of antiparallel β-sheets, previously detected in the capsid proteins of other icosahedral viruses. Two scenarios are considered as the basis for the conformational change that accompanies expansion: in the first, the changes are confined mainly to an (initially) highly α-helical gp23-Δ domain and involve a relatively minor refolding of gp23* in which about 30 residues are affected; in the second, gp23-Δ is not affected disproportionately, and refolding of gp23* occurs on a much larger scale, whereby 60-70 residues change their secondary structures.

The bacteriophage T4 capsid is first assembled as a precursor particle (prohead) that is ~18% smaller in scale than the mature capsid. The prohead contains the full complement of the major capsid protein, appropriately arranged in a prolate icosahedral surface lattice [reviews in Eiserling (1983) and Black and Showe (1983)]. This protein, gp23 (521 amino acids of known sequence; Parker et al., 1984), is present in the mature capsid in a proteolytically modified form, gp23*, with 65 residues (the so-called Δ-region, or gp23-Δ) removed from its amino terminus (Tsugita et al., 1975; Parker et al., 1984). After completion of assembly, the prohead undergoes a radical structural transformation which is responsible not only for the increased size of the mature capsid but also for the other striking differences—structural, functional, and immunological—between it and the prohead capsoid [reviews in Kellenberger (1980), Steven (1981), and Casjens and Hendrix (1988)]. This maturation-dependent capsid expansion appears to be a generic feature, common to the assembly pathways of most if not all icosahedral dsDNA phages. However, proteolysis of the major capsid protein is not a universal prerequisite for capsid expansion, occurring in some systems (e.g., T-even, P2) but not others (e.g., λ, P22, T3/T7). Functionally, this expansion transformation confers the following advantages: (1) it stabilizes the relatively labile prohead against breakdown either by dissociating conditions encountered in the environment or by internal pressure exerted by packaged DNA; (2) it greatly increases the internal capacity for DNA, by ~65%; (3) it drives the head-assembly reaction toward the accumulation of more complete particles (Ross et al., 1985).

The physical basis of this transformation is a massive and irreversible conformational change undergone by the proteins arrayed in the prohead surface lattice. Considered as a folding/refolding phenomenon of the gp23/gp23* molecules, there are three distinct mechanisms that may—theoretically, at least—underlie such a conformational change [cf. Rossmann and Erickson (1985)]: (i) the relative movement (mutual rotation and/or translation) of domains whose structures remain essentially unchanged; (ii) an order–disorder transition in which part of the polypeptide chain converts from a specific conformation to a disordered (unfolded) state, or vice versa: and (iii) refolding of the polypeptide chain into a specific conformation that is different from its original state.

The technique of laser Raman spectroscopy (Thomas et al., 1982; Thomas, 1986) has the potential to distinguish between the three types of mechanism noted above, since it has the capability to make quantitative measurements of secondary structure of proteins in large complexes (Williams & Dunker, 1981; Williams, 1983, 1986), and all three mechanisms make specific and different predictions as to how the secondary structure should change in the expansion transformation. According to mechanism i, which has been advocated to underlie phage capsid expansion (Kistler et al., 1978; Casjens, 1979; King, 1981), changes in secondary structure should be

† This work was funded in part by the Strategic Defense Initiative Organization Medical Free Electron Laser Program at USUHS, Grant GM7160, to R.W.W. In this context, the opinions and assertions contained herein are the private ones of the authors and are not to be construed as officially reflecting the views of the Department of Defense or the Uniformed Services University of the Health Sciences.

* Correspondence should be addressed to this author at Building 6, Room 114, National Institutes of Health, Bethesda, MD 20892.

‡ National Institute of Arthritis, Musculoskeletal and Skin Diseases.

§ Uniformed Services University of the Health Sciences.

Table I: Secondary Structure Contents (%) of the Major Capsid Protein of Bacteriophage T4 in Various Conformational States Calculated from the Raman Amide I and Amide III Spectra[a]

protein	amide I				amide III			
	α-helix	β-sheet	β-turn	N	α-helix	β-sheet	β-turn	N
precursor polyheads (gp23, unexpanded)	37 ± 3	34 ± 1	16 ± 1	3	38 ± 2	32 ± 3	19 ± 1	3
mature polyheads (gp23*, expanded)	21 ± 2	43 ± 3	19 ± 3	3	24 ± 1	47 ± 1	19 ± 0	2
Gdn-treated polyheads (gp23, expanded)	19 ± 2	47 ± 1	21 ± 2	3	26 ± 1	48 ± 4	17 ± 1	2
thermally denatured precursor polyheads	2	64	21	1	10	62	19	1
thermally denatured mature polyheads	1	62	21	1	9	63	20	1
exptl uncertainty	±4	±3	±2		±5	±6	±5	

[a] These numbers represent the average values and standard deviations for sets of N measurements, each of which relates to an independent preparation of polyheads. The remainder (to 100%) is undefined structure. The experimental uncertainty quoted for each secondary structure measurement is the standard deviation of the discrepancy between the structures of the reference set of proteins as given by high-resolution X-ray crystallography, and as calculated from their Raman spectra (Williams, 1986).

very slight, being confined to the small minority of residues sited in interdomainal hinge regions. Mechanisms ii and iii, on the other hand, anticipate substantial changes in secondary structure, which, in case ii, would entail an altered amount of undefined structure (unfolded state).

In the present study, we have analyzed the Raman spectra of purified polyheads, which are tubular polymorphic variants of the icosahedral capsid (Yanagida et al., 1970). For present purposes, polyheads have the advantage of being devoid of the other capsid proteins, which, if present, would impede inferences as to the conformational states of gp23/gp23*. Polyheads related to the prohead ("precursor" polyheads, with uncleaved gp23 and an unexpanded surface lattice) are assembled in vivo in the event of defects in any of several genes responsible for directing prohead assembly (Epstein et al., 1963; Steven et al., 1976a). Moreover, such polyheads may be processed in vitro into "mature" polyheads (gp23*, expanded surface lattice), simulating the transformation undergone by the maturing capsid (Steven et al., 1976b; Laemmli et al., 1976). Thus, we have analyzed the Raman spectra of precursor and mature polyheads, as well as polyheads containing uncleaved gp23 which were induced to expand in vitro.

Materials and Methods

(*a*) *Preparation of Polyheads.* Precursor and mature polyheads were prepared according to Steven et al. (1976b) and Ross et al. (1985), with a few modifications (Steven et al., unpublished results). In brief, they were prepared as follows:

(*i*) *Precursor polyheads* were produced by growing the mutant T4.22(amE209) in *Escherichia coli* B^E. The purification procedure described by Ross et al. (1985) was supplemented by a final step in which the polyheads were centrifuged through a sucrose/CsCl step gradient. The polyhead-containing fraction was then dialyzed against SCB buffer (0.1 M $KHPO_4$, 1 mM $MgSO_4$, pH 7.0) at 20 °C and then washed twice in the same buffer, by centrifugation followed by resuspension of the pellet in the same buffer.

(*ii*) *Mature polyheads* were produced by following the procedure of Ross et al. (1985), except that pronase E (Sigma, St Louis, MO) at 0.25 μg/mL was added to the lysate. Finally, after the expanded polyheads had been isolated and subjected to "SDS cleaning" (Steven et al., 1976b), residual amounts of incompletely cleaved gp23 were converted to gp23* by incubation for 1 h at 37 °C in the presence of 0.1 mg/mL trypsin (Sigma, St Louis, MO).

(*iii*) *Uncleaved, expanded polyheads* were produced as follows: Drops of 2.5 M guanidine hydrochloride (Gdn·HCl) were added to a suspension of purified precursor polyheads (1.5 mg/mL protein in SCB) at room temperature (~20 °C), to a final concentration of 0.25 M Gdn·HCl. Phenylmethanesulfonyl fluoride (PMSF) was added, to 1 mM. The polyheads were incubated for 30 min, transferred to 4 °C for 3 h, and then dialyzed against 10 mM potassium phosphate, pH 7.0, for 2 h at 4 °C, with one change of dialysis buffer. Finally, the sample was centrifuged (18 000 rpm, Sorvall SS-34, 40 min, 4 °C) and the pellet overlaid with a small volume of SCB, allowed to resuspend overnight, and finally diluted to the desired concentration in SCB. The resulting preparation was routinely assayed by SDS–PAGE of boiled and unboiled samples, and by negative staining electron microscopy.

(*b*) *SDS–polyacrylamide gel electrophoresis*, using either 10% or 12.5% polyacrylamide gels, was performed according to standard procedures (Maizel, 1971). Proteins were detected by staining with Coomassie Brilliant Blue R-250.

(*c*) *Electron Microscopy and Optical Diffraction.* Negative staining with uranyl acetate and observation of the resulting specimens with a Philips EM400T electron microscope were performed according to Ross et al. 1985). Visual inspection and photographic recording of optical diffraction patterns from electron micrograph negatives were performed with a folded-beam diffractometer, according to Steven and Navia (1980). In comparing the lattice constants of polyheads expanded in vitro with those of unexpanded controls, reciprocal lattice constants were measured from the optical diffraction patterns of at least 12 particles of both kinds, averaging over the three directions of the hexagonal lattice in each case. The standard deviations were of the order of 1% in both cases.

(*d*) *Laser Raman Spectroscopy.* The visible Raman instrument and data analysis have been described previously (Williams, 1986; Williams & Beeler, 1986). Amide I spectra were analyzed for secondary structure content by using the singular value decomposition method. Amide III spectra were analyzed by using least-squares solutions constrained to nonnegative values.

Results

Laser Raman Spectroscopy of Precursor and Mature Polyheads. Polyheads of both types were prepared according to established procedures. The purity and homogeneity of each batch were confirmed by SDS–PAGE and electron microscopy. Freshly prepared polyheads were centrifuged into a pellet, which was taken up in a glass melting point capillary and analyzed by laser Raman spectroscopy. From the resulting data, a determination of the secondary structure of gp23 (and gp23*, respectively) was performed. Representative spectra are shown in Figure 1, and the quantitations of secondary structure are compiled in Table I.

The data reproducibly show that a substantial change in secondary structure takes place between these successive states of the surface lattice. Marked differences are evident between

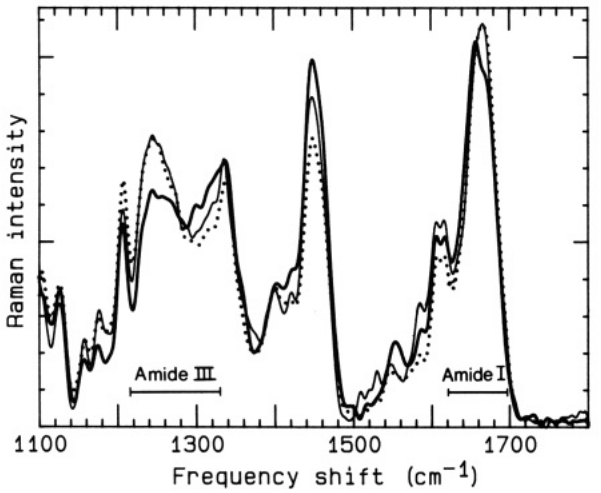

FIGURE 1: Laser Raman spectra of (thick continuous line) precursor polyheads, i.e., uncleaved gp23, unexpanded surface lattice; (dotted line) mature polyheads, i.e., gp23*, expanded surface lattice; and (thin continuous line) precursor polyheads treated with 0.25 M Gdn·HCl, i.e., uncleaved gp23, expanded surface lattice. The spectra of the two expanded lattices (cleaved and uncleaved) resemble each other closely and are distinctly different from the spectrum of the unexpanded surface lattice.

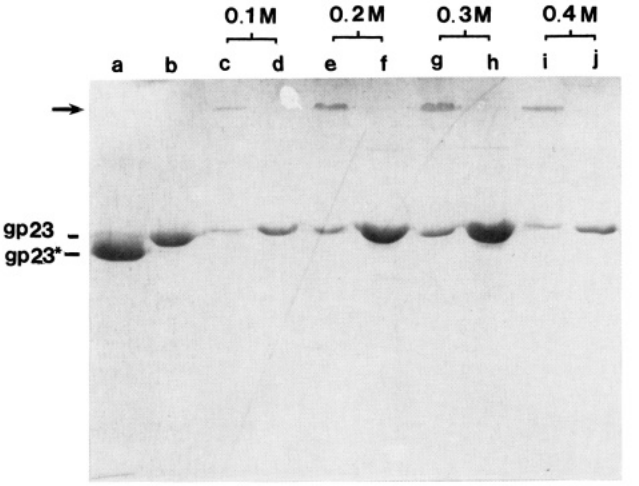

FIGURE 2: SDS–polyacrylamide gel showing samples of precursor polyheads that had been incubated in the presence of increasing concentrations of Gdn·HCl. For each specimen, a sample in SDS-containing gel buffer was loaded on the gel without boiling (c, e, g, i) and after boiling for 3 min (d, f, h, j). The unboiled samples contain an additional minor band of higher molecular weight (arrow), presumably an undissociated oligomer of gp23. (a) and (b) are markers for gp23* and gp23, from preparations of mature and precursor-type polyheads, respectively; both of the latter samples were boiled.

the shapes of the respective spectra in both the amide I and the amide III regions (Figure 1). These differences are reflected in quantitative changes in the secondary structures calculated from the spectra. In precursor polyheads, gp23 has approximately equal contents of α-helix and β-sheet—about one-third of the residues in each case. In contrast, the α-helix content of the mature polyheads is greatly reduced (by 14–16%), whereas their β-sheet content is increased by 9–15% (Table I). These differences were reproducibly observed in analyses of independent preparations, the standard deviations for all secondary structure components, from experiment to experiment, being no greater than 2–3%. Moreover, the same results emerged consistently from the analyses of both the amide I and the amide III bands. The estimated accuracy of these measurements is at the level of 2–4% (amide I) and 5–6% (amide III), respectively (Table I). Relative to these margins of experimental error, therefore, the observed changes in secondary structure are highly significant.

These results strongly suggest that the expansion transformation involves a refolding of part of the gp23* polypeptide chain. However, this interpretation is clouded by the consideration that the gp23-Δ moiety of gp23 is missing from gp23*. If gp23-Δ were to be entirely α-helical—an extreme case—then one can calculate that the secondary structure of the remainder of gp23 (i.e., its gp23* moiety) should be 28% α-helix and 39% β-sheet in order to account for the amide I data in Table I. In terms of this scenario, the secondary structure change in gp23* upon expansion would be much less pronounced, amounting to a small decrease in α-helix content and a small increase in β-sheet. In order to resolve this issue—i.e., whether the observations are accounted for by a relatively large-scale conformational change in gp23*, or by a much smaller such change, together with the proteolytic removal of an α-helical gp23-Δ—we attempted to produce expanded polyheads that contain uncleaved gp23.

In Vitro Expansion of Uncleaved Polyheads. Since it has previously been shown that exposure to appropriate concentrations of denaturants may induce phage proheads to expand in vitro—4 M urea in the case of λ proheads (Kuenzler & Hohn, 1978) and 0.8% SDS for P22 proheads (Earnshaw et al., 1976), we tried exposing freshly prepared precursor polyheads to such reagents. Our experimental assay was based on the observation that expanded polyheads are not dissociated by 1% SDS at 20 °C, whereas unexpanded polyheads are readily dissociated under these conditions (Steven et al., 1976b). Accordingly, assuming that gp23-containing expanded polyheads would share this property, they should be identifiable as such by comparing boiled and unboiled samples by SDS–PAGE, since their protein will only enter the gel in the boiled sample. The most successful results were obtained with 0.2–0.3 M Gdn·HCl (Figure 2). At lower concentrations, rather little protein enters the gel with or without boiling (Figure 2c,d), indicating that the polyheads were not affected by the reagent and, being still unexpanded, dissociated for the most part under the low ionic strength wash conditions used in this experiment (Van Driel, 1977). At higher concentrations of Gdn·HCl, the denaturant apparently causes dissociation rather than expansion of the polyheads, since again, a rather low yield of protein is detected on the gel (Figure 2i,j).

Polyheads rendered insoluble in cold SDS by exposure to 0.25 M Gdn·HCl were examined by negative staining electron microscopy (Figure 3a,b), and their hexagonal lattice constants were measured by optical diffraction (Figure 3c). The ratio between their average lattice constant and that of unexpanded control polyheads from the same preparation was 1.193 ± 0.025 (n = 20 for both sets of measurements), confirming that the lattice expansion had indeed taken place.

These results may be compared with the earlier observations that the prohead-like particles, mainly morphologically aberrant, assembled under nonpermissive conditions by the mutant 23(tsA78) undergo expansion in vivo without cleavage and that polyheads produced by the 23(tsA78).21(tsN8) double mutant have expanded surface lattices (Onorato et al., 1978). However, we are aware of no cases in which capsid-related particles composed of wild-type gp23 undergo expansion in vivo in the absence of cleavage. Thus, although expansion of the uncleaved surface lattice does not normally occur in vivo in the T4 system, it may be induced in vitro and is expedient for these experiments.

Laser Raman Spectroscopy of Uncleaved, Expanded Polyheads. After thorough washing by dialysis and centrifugation to ensure that the spectra would not be affected by

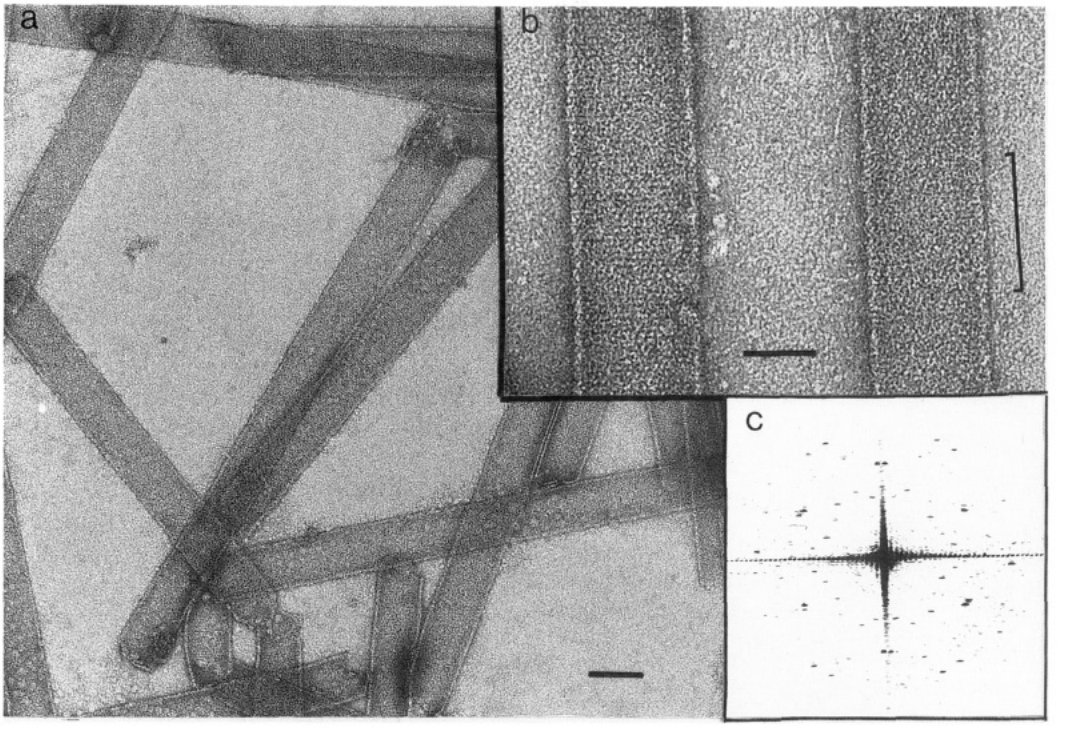

FIGURE 3: (a) Electron micrograph of uncleaved polyheads after treatment with 0.25 M Gdn·HCl, negatively stained with uranyl acetate. Their surface lattice morphology is shown at higher magnification in panel b. An optical diffraction pattern of the polyhead segment marked in panel b is shown in panel c. Its periodic reflections index on a double hexagonal reciprocal lattice, whose periodicity (14.0 nm) is characteristic of the expanded state of the capsid.

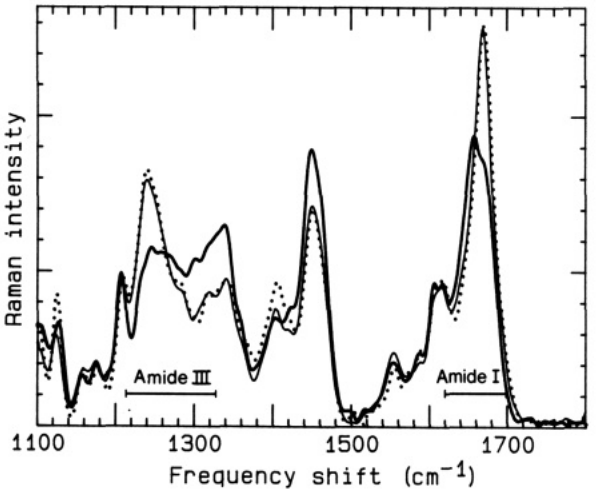

FIGURE 4: Laser Raman spectra of precursor polyheads before (thick continuous line) and after (thin continuous line) thermal denaturation at 70 °C. Also shown is the spectrum of thermally denatured mature polyheads (dotted line) after incubation at 85 °C, which is virtually identical with that of thermally denatured precursor polyheads.

any residual traces of Gdn·HCl, these polyheads were analyzed in essentially the same manner as the other samples. The resulting spectra (e.g., Figure 1) and secondary structure calculated from them (Table I) are very similar to those of **cleaved** expanded polyheads.

Secondary Structure of Thermally Denatured Polyheads. It has previously been established that "precursor" polyheads undergo thermal denaturation at 65 °C, whereas "mature" polyheads denature at 75–80 °C (Ross et al., 1985). Thermally denatured polyheads provide a "benchmark" for the expansion transformation in that they represent a major, albeit nonphysiological, conformational change of gp23 and gp23*. Accordingly, precursor polyheads were incubated at 70 °C and then cooled to room temperature and analyzed by laser Raman spectroscopy (Figure 4 and Table I). Their secondary structure is essentially devoid of α-helices and has a greatly enhanced β-sheet content (Table I), presumably indicative of the secondary structure assumed by the "malnatured" protein after irreversible thermal denaturation. Similar secondary structure is detected in malnatured gp23*, after incubation of mature polyheads at 85 °C (Table I).

Table II: Conformational Predictions for gp23, gp23*, and gp23-Δ in Percentages of Total (and Numbers of Residues)

	% of total (no. of residues)			
protein	α-helix	β-sheet	β-turn	undefined
gp23 (521)	35 (182)	18 (94)	22 (115)	25 (140)
gp23* (456)	32 (145)	20 (91)	23 (106)	25 (114)
gp23-Δ (65)	57 (37)	5 (3)	14 (9)	25 (16)

[a] Predictions were made according to Williams et al. (1987), with no constraints from the measured conformational content. The correlation coefficient between predictions made with this method for 75 proteins with their conformational contents determined by X-ray crystallography is 0.63.

Discussion

Gp23/Gp23 May Contain a Domain with the β-Barrel Motif Found in Other Capsid Proteins.* Analysis of the laser Raman spectrum of the mature gp23* surface lattice reveals a substantial fraction (~45%) of β-sheet. It is noteworthy that the capsid proteins of the small icosahedral RNA plant and animal viruses whose structures have been solved to high resolution by X-ray crystallography all have high contents of β-sheet. Their foldings conform to a characteristic "β-barrel" motif, based on eight strands of antiparallel β-sheets [see Rossmann and Erickson (1985)]. Moreover, adenovirus, a dsDNA animal virus of much greater size and complexity, has a major capsid protein that contains two copies of essentially the same motif (Roberts et al., 1986). Noting the large β-sheet contents of gp23* or gp23 in the expanded surface lattice—

some 200 residues (Tables I and II)—(and even that of gp23 in the unexpanded state), it is tempting to conjecture that these proteins may also contain a domain with this archetypal capsid protein fold, or variant thereof. However, since such a domain would account for less than half of their molecular weights, it follows that gp23 and gp23* should also contain other structural elements not present in the smaller capsid proteins of these spherical RNA viruses.

Spectroscopic Investigations of the Expansion Transformations of Other Phage Capsids. Laser Raman spectroscopy was first used to investigate the expansion of bacteriophage capsids by Thomas et al. (1982), who examined the prohead and the mature capsid of P22, as well as several other particles, including proheads whose scaffolding cores had been removed by treatment with 1 M Gdn·HCl. Their findings differ from those of the present study in that (i) they detected smaller fractions of regular secondary structure in the P22 prohead (20% α-helix, 25% β-sheet) and (ii) comparison of the Raman spectra of capsids and emptied proheads led them to conclude that any change in the capsid protein's secondary structure should be slight, affecting less than 10% of residues, their estimated threshold of detectability.

There are, however, significant differences—procedural as well as biochemical—between that study and the present one. The method used by Thomas et al. (1982) for determining secondary structure from Raman spectra (Lippert et al., 1976) is less precise than that used here. Perhaps more importantly, the major capsid protein accounts for only about 70% of the P22 prohead mass, the remainder being mostly its scaffolding protein. This protein was removed by treating proheads with 1 M Gdn·HCl (Thomas et al., 1982). For reference, P22 proheads are dissociated at 2–3 M Gdn·HCl, and their proteins remain soluble in 1.5 M Gdn·HCl (Fuller & King, 1981). Thus, although Fuller and King (1981) allude to preliminary X-ray diffraction experiments, it does not appear to have been established conclusively that P22 proheads are not expanded by exposure to 1 M Gdn·HCl (as they are, for instance, by treatment with 0.8% SDS; Earnshaw et al., 1976). If 1 M Gdn·HCl were to induce expansion, emptied proheads and capsids would represent the same conformational state, and no difference between their spectra would be expected.

Kawaguchi et al. (1983) have studied the expansion of λ proheads, as induced by 4 M urea, by circular dichroism and fluorescence measurements. They found that the secondary structure (estimated as 29% α-helix and 23% β-structure) showed little evidence of change upon expansion, although several Tyr residues were found to be transferred from a polar to a nonpolar environment. On this basis, they concluded that the expansion involves mainly interdomainal movements of the capsid protein.

With the qualifications noted above, the earlier spectroscopic data relating to the capsid expansions of phages P22 and λ have yielded few indications of changes in secondary structure, although they do not appear to rule out such an effect, at least at the level of 10% or so. Although the similarities between the respective expansions imply the likelihood of a common molecular mechanism, there are noteworthy differences between T4, on the one hand, and P22 and λ, on the other. In particular, the roles of proteolytic cleavage and the gp23-Δ domain in the T4 system have no counterparts in P22 or λ.

Capsid Expansion of Icosahedral Plant Viruses. Another conformational change affecting viral capsids—the Ca^{2+}-regulated expansion of tomato bushy stunt virus (TBSV) and related plant viruses—has been studied in detail by X-ray crystallography (Robinson & Harrison, 1982). Comparing

Table III: Changes per Capsid Protein Subunit in Numbers of Residues of α-Helix and β-Sheet upon Expansion of T4 Precursor-Type Polyheads, Calculated from Raman Spectra

	amide I		amide III	
end state[a]	α-helix	β-sheet	α-helix	β-sheet
cleaved, expanded	−97	+19	−89	+47
uncleaved, expanded	−94	+68	−63	+83

[a] Gp23 has 521 residues (Parker et al., 1984), of which the N-terminal 65 (gp23-Δ) are removed upon cleavage to gp23* (456 residues).

maps at 0.8-nm resolution for the expanded state and 0.3-nm resolution for the contracted state, they concluded that this transition represents primarily a swiveling of conserved domains. However, the plant virus capsid expansion is functionally very different from phage capsid expansion in that it destabilizes the capsid structure and is thus implicated in releasing the viral RNA inside the infected cell. In contrast, the T4 capsid expansion results in a much more stable structure.

Secondary Structure Predictions: Implications for gp23-Δ. Although conscious of the limitations of predictive schemes (Kabsch & Sander, 1983), particularly when confronted with two quite different conformational states of the same protein, we have nevertheless evaluated the sequences of gp23, gp23*, and gp23-Δ according to the procedure of Williams et al. (1987) (Table II). The α-helix prediction for gp23 is consistent with the experimental measurement, but there is a substantial shortfall in the β-sheet prediction. Gp23-Δ is predicted to have a higher fraction of α-helix than gp23 as a whole, and virtually no β-sheets. This prediction is reminiscent of the hypothesis formulated above (Results) as a way to explain the observed difference between precursor and mature polyheads without having to invoke large-scale refolding of gp23*. A variant of this hypothesis might now be considered to account for the difference between the spectra of unexpanded and expanded gp23-containing polyheads, which minimizes the extent to which a refolding of their gp23* moieties is required. If the transition were to involve denaturation of gp23-Δ, whereby its α-helices were converted into β-sheets (as, in fact, happens with heat-denatured gp23 and gp23*), this would account for much of the observed effect.

Scale of Conformational Change: Fraction of Residues Involved. On the basis of this Raman spectral analysis, we conclude that the expansion transformation of the T4 major capsid protein involves a substantial change in secondary structure, dominated by a major reduction in α-helix content, accompanied by an increase in β-sheet. Our best estimates of the numbers of residues involved are given in Table III. Although the data do not extend to identification of the segments of gp23 that undergo refolding in these transitions, we have focused on two "extreme case" scenarios. The first attributes the observed changes, in large part, to an almost completely α-helical gp23-Δ domain that is excised and removed in the case of cleavage preceding expansion, and converted mainly into β-sheets when the uncleaved lattice is expanded in vitro. According to this scenario, the gp23* portion of the molecule is minimally affected, although it should sustain some loss of α-helix to the extent of about 30 residues, and a comparable increase in β-sheet (cf. Table III). The second scenario envisages that gp23-Δ is not affected disproportionately, and thus invokes refolding on a considerably larger scale in gp23*, i.e., the loss of 60–70 residues of α-helix, with a comparable number of residues switching to β-sheet. Also viable are scenarios that are intermediate between these two extremes in the relative weightings that they assign to gp23-Δ and gp23* in accounting for the observed effects.

It should, however, be stressed that the observed **increase** in the absolute number of residues per gp23* subunit in β-sheet conformation in the cleaved expanded state (Table III) cannot be attributed to the gp23-Δ domain. Accordingly, refolding on a significant scale, affecting at least 30 residues or so, does take place in the gp23* portion of T4 capsid protein upon expansion.

Conformational Transitions in Other Proteins and Peptides. In reviewing pertinent observations from other viral capsid proteins (above), we find no precedent for a comparably radical conformational change. However, there have been a number of reports of transitions affecting peptide hormones that involve switching between α-helical and other conformations, albeit on a much smaller scale than the expansion-dependent conformational change of gp23/gp23*. For instance, a change in the Zn-binding status of the insulin hexamer is accompanied by the switching of $\sim$9 residues from an α-helical to an extended conformation (Renscheidt et al., 1984). Similarly, Rosenblatt et al. (1980) detected an enhancement of α-helix and elimination of β-sheets in a synthetic peptide corresponding to part of the preproparathyroid hormone when transferred from an aqueous buffer to a nonpolar solvent.

It is also noteworthy that recent crystallographic studies of phosphofructokinase have shown that the allosteric transition of this enzyme involves unfolding of a full turn of α-helix (Janin, 1989; Rypniewski & Evans, 1989). The consideration that the T4 capsid expansion is irreversible, unlike the enzyme which must cycle between two states, may allow it to deploy a similar conformational rearrangement on a much larger scale.

ACKNOWLEDGMENTS

We thank Dr. L. W. Black for helpful advice and discussions, Ms. M. E. Bisher for help with electron microscopy and photography, and Dr. G. J. Thomas for exchanging information prior to publication.

REFERENCES

Black, L. W., & Showe, M. K. (1983) in *Bacteriophage T4* (Mathews, C. K., Kutter, E. M., Mosig, G. & Berget, P. B.) pp 219–245, American Society for Microbiology, Washington, DC.

Casjens, S. (1979) *J. Mol. Biol. 131*, 1–19.

Casjens, S., & Hendrix, R. (1988) in *The Bacteriophages* (Calendar, R., Ed.) Vol. 1, pp 15–91, Plenum Publishing Corp., New York.

Earnshaw, W., Casjens, S., & Harrison, S. C. (1976) *J. Mol. Biol. 104*, 387–410.

Eiserling, F. A. (1983) in *Bacteriophage T4* (Mathews, C. K., Kutter E. M., Mosig, G., & Berget, P. B.) pp 11–24, American Society for Microbiology, Washington, DC.

Epstein, R. H., Bolle, A., Steinberg, C., Kellenberger, E., Boy de la Tour, E., Chevalley, R., Edgar, R., Susman, M., Denhardt, C., & Lielausis, I. (1963) *Cold Spring Harbor Symp. Quant. Biol. 28*, 375–392.

Fuller, M. T., & King, J. (1981) *Virology 112*, 529–547.

Janin, J. (1989) *Nature (London) 339*, 261–262.

Kabsch, W., & Sander, C. (1983) *FEBS Lett. 155*, 179–182.

Kawaguchi, K., Noda, H., & Katsura, I. (1983) *J. Mol. Biol. 164*, 573–587.

Kellenberger, E. (1980) *Biosystems 12*, 201–223.

King, J. (1981) in *Biological Regulation and Development* (Goldberger, R. F., Ed.) pp 101–132, Plenum Publishing Corp., New York.

Kistler, J., Aebi, U., Onorato, L., Ten Heggeler, B., & Showe, M. K. (1978) *J. Mol. Biol. 126*, 571–589.

Kuenzler, P., & Hohn, T. (1978) *J. Mol. Biol. 126*, 571–589.

Laemmli, U. K., Amos, L. A., & Klug, A. (1976) *Cell 7*, 191–203.

Lippert, J. L., Tyminski, D., & Desmeules, P. J. (1976) *J. Am. Chem. Soc. 98*, 7075–7080.

Maizel, J. V. (1971) *Methods Virol. 5*, 179–246.

Onorato, L., Stirmer, B., & Showe, M. K. (1978) *J. Virol. 27*, 409–426.

Parker, M. L., Christensen, A. C., Boosman, A., Stockard, J., Young, E. T., & Doermann, A. H. (1984) *J. Mol. Biol. 180*, 399–416.

Renscheidt, R., Strassburger, W., Glatter, U., Wollmer, A., Dodson, G. G., & Mercola, D. A. (1984) *Eur. J. Biochem. 83*, 1268–1275.

Roberts, M. M., White, J. L., Gruetter, M. G., & Burnett, R. M. (1986) *Science 232*, 1148–1151.

Robinson, I. K., & Harrison, S. C. (1982) *Nature (London) 297*, 563–568.

Rosenblatt, M., Beaudette, N. V., & Fasman, G. D. (1980) *Proc. Natl. Acad. Sci. U.S.A. 77*, 3983–3987.

Ross, P. B., Black, L. W., Bisher, M. E., & Steven, A. C. (1985) *J. Mol. Biol. 183*, 353–364.

Rossmann, M. S., & Erickson, J. W. (1985) in *Virus Structure and Assembly* (Casjens, S., Ed.) pp 29–74, Jones & Bartlett, Boston.

Rypniewski, W. R., & Evans, P. R. (1989) *J. Mol. Biol. 207*, 805–821.

Steven, A. C. (1981) in *Methods in Cell Biology: Three-Dimensional Ultrastructure in Biology* (Turner, J. N., Ed.) Vol. 22, pp 298–324, Academic Press, New York.

Steven, A. C., & Navia, M. A. (1980) *Proc. Natl. Acad. Sci. U.S.A. 77*, 4721–4725.

Steven, A. C., Aebi, U., & Showe, M. K. (1976a) *J. Mol. Biol. 102*, 373–407.

Steven A. C., Couture, E., Aebi, U., & Showe, M. K. (1976b) *J. Mol. Biol. 106*, 187–221.

Thomas, G. J. (1986) in *Spectroscopy* of *Biological Systems* (Clark, R. J. H., & Hester, R. E., Eds.) pp 233–309, John Wiley & Sons, New York.

Thomas, G. J., Yi, Y., Fuller, M. T., & King, J. (1982) *Biochemistry 21*, 3866–3878.

Tsugita, A., Black, L. W., & Showe, M. K. (1975) *J. Mol. Biol. 98*, 271–275.

Van Driel, R. (1977) *J. Mol. Biol. 114*, 61–72.

Williams, R. W. (1983) *J. Mol. Biol. 166*, 581–603.

Williams, R. W. (1986) in *Methods* in *Enzymology: Enzyme Structure* (Hirs, C. H. W., & Timasheff, S. N., Eds.) Vol. 130, pp 311–331, Academic Press, New York.

Williams, R. W., & Dunker, A. K. (1981) *J. Mol.* Biol. *152*, 783–813.

Williams, R. W., & Beeler, T. J. (1986) *J. Biol. Chem. 261*, 12408–12413.

Williams, R. W., Chang, A., Juretic, D., & Loughtran, S. (1987) *Biochim. Biophys. Acta 916*, 200–204.

Yanagida, M., Boy de la Tour, E., Alff-Steinberger, C., & Kellenberger, E. (1970) *J. Mol. Biol. 50*, 35–58.